CROSS SECTIONS FOR l-MIXING OF K(n^2F) STATES IN COLLISIONS WITH GROUND-STATE K(4^2S) ATOMS

M. GŁÓDŹ[a,*], A. HUZANDROV[a], J. KLAVINS[b], I. SYDORYK[a], J. SZONERT[a], S. GATEVA-KOSTOVA[c] AND K. KOWALSKI[a,d]

[a]Institute of Physics, Polish Academy of Sciences
Al. Lotników 32/46, 02-668 Warszawa, Poland
[b]Institute of Atomic Physics and Spectroscopy, University of Latvia, Riga, 1586, Latvia
[c]Institute of Electronics, BAS, 1784 Sofia, Boul. Tsarigradsko Shosse 72, Bulgaria
[d]College of Science, Al. Lotników 32/46, 02-668 Warszawa, Poland

(Received August 3, 2000)

We report measurements of the cross sections $\sigma_{l-\mathrm{mix}}$ for angular momentum mixing of the K(n^2F) (n = 6, 7, 8) states with the K($n, l > 3$) states, induced in thermal collisions with parent ground state K(4^2S) atoms. The experiment was performed in a cell heated to *ca.* 450 K. The n^2F states were excited in two steps: $4^2S \rightarrow 4^2P \rightarrow n^2F$ by using a diode laser for the first step (a dipole-transition) and a pulsed dye laser for the second step (a quadrupole-transition). The measured values $\sigma_{l-\mathrm{mix}}(6^2F) = 3.6 \pm 2.2$, $\sigma_{l-\mathrm{mix}}(7^2F) = 4.2 \pm 2.6$ and $\sigma_{l-\mathrm{mix}}(8^2F) = 8.0 \pm 4.6$ (in units of 10^{-13} cm^{-1}) are close to the corresponding values of the geometrical cross sections.

PACS numbers: 34.50.Fa

1. Introduction

Quenching of the alkali metal n^2F states induced by thermal collisions with parent ground state atoms was investigated experimentally in Rb for $9 \leq n \leq 21$ by Hugon et al. [1] and in Cs for $n = 7 \div 11$ by Marek and Ryschka [2]. While all the l states of the same n are degenerate for hydrogen, for heavier alkali atoms (Cs, Rb, and also K) only states $l \geq 3$ are nearly degenerate (quasi-hydrogenic), as characterised by small quantum defects $\delta_l = n - n_l^*$. For Na and Li such states are $l \geq 2$. Besides these two experiments on self-quenching of quasi-hydrogenic alkali states, a number of studies have been performed on quenching of such states by inert gas atoms, e.g. Na(n^2D)+He, Ne, Ar, for $n = 6 \div 15$ (for Ar also for

*corresponding author, e-mail: glodz@ifpan.edu.pl

$n = 5$) [3]; Na(n^2F)+He, Ne, Ar, for $n = 13 \div 15$ [4]; Rb(n^2F)+He, Ar, Xe for $9 \leq n \leq 21$ [1] and for $n \geq 20$ [5, 6]. Experiments aimed at the transfer $4^2D \rightarrow 4^2F$ in collisions with parent atoms and noble gas atoms in Li [7] and in Na [8] should also be mentioned.

The energy separation between a given quasi-hydrogenic alkali (n, l) state and any other quasi-hydrogenic (n, l') state is much smaller than the separation between (n, l) and any other state of the atom. It can be therefore expected then that, as a result of a collision with a perturber, population from the (n, l) state is transferred almost entirely to the nearby angular momentum l' states. Early studies [1, 3] verified the expectations concerning the final products of quenching, and collisional quenching of a quasi-hydrogenic alkali state has been identified with this process of angular momentum transfer, for which the term l-mixing was coined in Ref. [3].

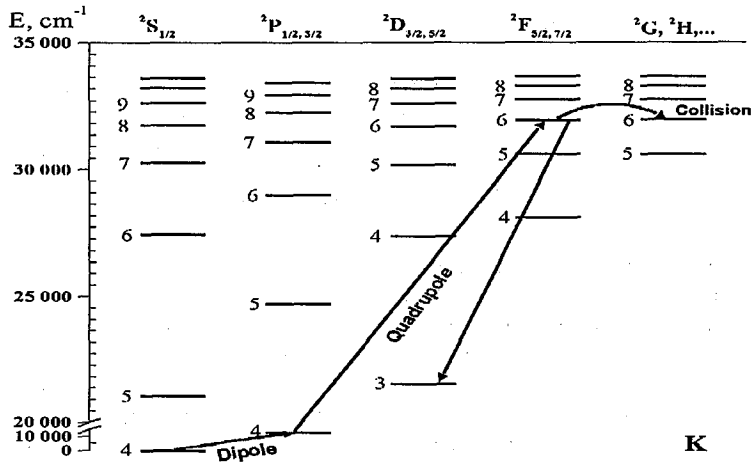

Fig. 1. Potassium levels; dipole–quadrupole excitation of the K(6^2F) state, collisional l-mixing and observed fluorescence transition are marked by arrows.

The lack of respective data for potassium inspired us to carry out measurements of self-quenching of the K(n^2F) states (for $n = 6$, 7, 8). While separation between e.g. the K(6^2F) state and the other two $l > 3$ states, 6^2G and 6^2H (Fig. 1), is only *ca.* 8 cm^{-1}, separation between 6^2F and its closest ($n = 6, l < 3$) state, 6^2D, amounts to 257 cm^{-1}; and between 6^2F and its other two closest (n', l') states, 8^2S and 8^2P, is 188 cm^{-1} and 276 cm^{-1}, respectively. Analogous ordering and relative separations of the levels hold for the higher K(n^2F) states. It is therefore justified to assume that also the K(n^2F) states are dominantly quenched through the quasi-elastic l-mixing channels. Each channel can be described by the reaction

$$\mathrm{K}(n^2F) + \mathrm{K}(4^2S) \rightarrow \mathrm{K}(n, l > 3) + \mathrm{K}(4^2S) \tag{1}$$

and is characterised by the partial cross section $\sigma_{nF \rightarrow (n,l)}$. The total l-mixing cross section is the sum of the contributions

$$\sigma_{l-\mathrm{mix}}\left(\mathrm{K}(n^2F)\right) = \sum_{l=4}^{n-1} \sigma_{nF \rightarrow (n,l)}. \tag{2}$$

Consequently, we shall refer to our measured quenching cross sections as to cross sections for l-mixing, $\sigma_{l-\mathrm{mix}}$.

With a small energy exchange during (quasi-elastic) l-mixing, corresponding cross sections are large, as observed in the cited papers. For small n-values the cross sections sharply increase with n, then they saturate about $n^{\max}$, the value of which depends on the colliding partners, and ultimately start to decrease with n. Various theoretical papers were devoted to l-mixing, as reviewed in e.g. [9–11]. The collision is a complicated three-body process, since all three participants interact: the alkali metal atomic core, excited valence electron of this atom and the perturber atom. Yet it appeared that in many instances reasonable agreement with experiment was reached by treating thermal l-mixing collision in terms of a binary encounter of the neutral perturber with the valence electron, which is considered to be quasi-free (see e.g. in reviews [9, 10, 12, 13]). The possible influence of the other interactions, especially between the atomic core and the neutral perturber, was also investigated, as well as mutual interference of both contributions (e.g. [11] and the references therein). General prediction for l-mixing is that at small n values, of interest in our experiment, the cross sections increase roughly as n^4, that is as the geometrical size of the atom, i.e. the size of the "cloud" of the excited state electron. This relation found a simple qualitative interpretation in the picture of the e^--perturber interaction [3].

Theorists have been inspired predominantly by experiments in which inert gas atoms act as a perturber. In contrast, the theory of collisions of Rydberg atoms, when the perturber is an alkali metal atom, has not been developed as well [14]. The only explicit theoretical cross sections for l-mixing in alkali–alkali homonuclear collisions are presented for Rb in [1] as "private communication" and they were calculated by de Prunelé–Pascale within the framework of their model [15], in which only the e^--perturber interaction was assumed. Satisfactory agreement with experimental cross sections of [1] was reached.

2. Experimental set-up and procedure

The investigated $K(n^2F)$ states were excited selectively in a two-step scheme, analogous to the one used earlier in our laboratory for lifetime measurement in $Rb(n^2F)$ [16]. The electric-dipole transition $4^2S_{1/2} \rightarrow 4^2P_{3/2}$ was followed by the electric-quadrupole transition $4^2P_{3/2} \rightarrow n^2F_{5/2,7/2}$ [17]. A cw laser was used in the first step, and a pulsed laser in the second (Fig. 1). With such a scheme, the ^2F states are excited optically in a direct way. Most of the schemes, reviewed in [18], used by other authors for alkali ^2F states in similar experiments, rely on superradiant cascading and one of them on microwave mixing [1, 2, 4, 19, 20].

The experimental set-up is shown in Fig. 2. The investigated medium was vapour over metallic potassium in a spectroscopic cell made of 1720 Corning glass. Glass of this type was used for two reasons: (*i*) as an alkali resistant glass and (*ii*) because the penetration of atmospheric helium through the walls of such cell is much weaker than for a Pyrex glass cell of similar dimensions, heated to the same temperature. Thus, unlike the case of Pyrex cells [21, 22], the amount of atmospheric helium can be safely neglected as an impurity even after long periods

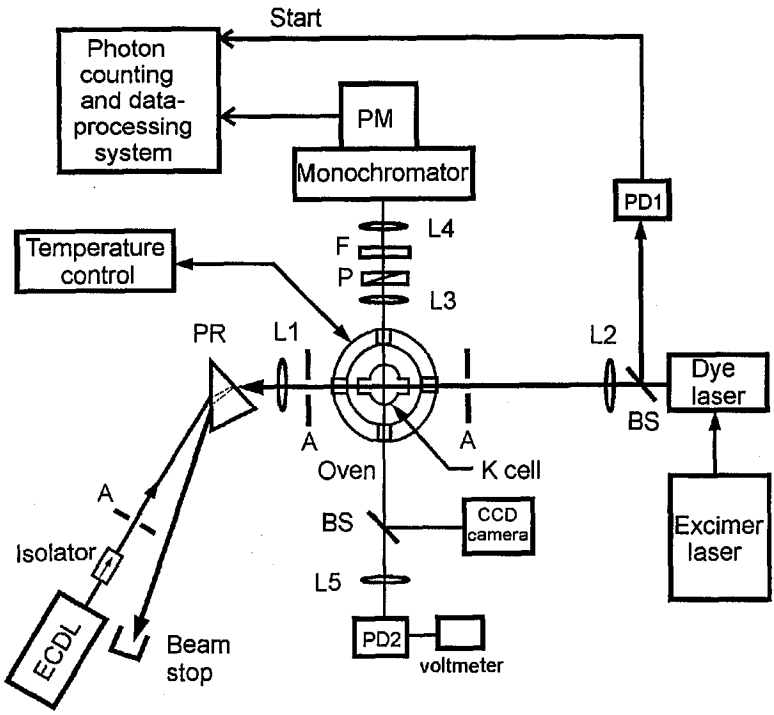

Fig. 2. The experimental set-up. ECDL — external cavity diode laser, PD1, PD2 — photodiodes, PR — prism, L1–L5 — lenses, A — aperture, BS — beam splitter, F — combined filters cutting off the scattered light from the lasers, P — polariser.

of operation at elevated temperatures. The cell was a cylinder (86 mm high, 25 mm dia) vaulted at both ends. Small windows attached to the sides allowed undistored input/output of the laser beams across the cylinder. The windows were supported on short tubes (10 mm dia) sealed to the cylinder in its upper part. Prior to filling with potassium, the cell was connected to a vacuum system and was well outgassed. It was heated with a gas torch and then baked in an oven for *ca.* one month, 2.5 weeks of which at *ca.* 900 K, until the base pressure of less than 1×10^{-8} Torr was reached. High purity potassium was then distilled into the cell and the cell was sealed off from the vacuum system.

During the experiment the cell was heated in a temperature controlled double chamber oven to near 450 K, which corresponds to number density of potassium of *ca.* 3.7×10^{13} cm^{-3} in the excitation region in the upper chamber. The Nesmeyanov temperature-vapour pressure relation was used [23]. The lower end of the cylinder was positioned in the lower chamber of the oven and was heated to a temperature of a few degrees below that of the upper part, to prevent condensation of potassium in the excitation region. The inside of the oven was shielded with a high permeability foil to reduce external magnetic fields due to the Earth and various laboratory sources.

The two counterpropagating laser beams were overlapped in the excitation region of the cell. They were partially focused to the diameter of *ca.* 0.5 mm at the centre of the oven. Before entering the cell windows they were made collinear by careful alignment. A number of irises were used to fix the beam positioning. A TUI OPTICS DL100 external cavity cw diode laser (ECDL), containing a FDL 770–20 laser diode with a DSYS DL 100 supply- and control-system, was used to excite the first step (dipole-)transition. The effective power at 766.5 nm was several mW. To reach this wavelength, it was necessary to cool the diode down to *ca.* 7°C. Although the diode was selected for the purpose of the experiment, its free running room temperature wavelength changed to a longer wavelength after some time of operation, probably because of ageing. A considerable temperature reduction was therefore necessary to reach efficient operation of ECDL at 766.5 nm. A 60 dB Gsänger DL1 optical isolator protected the laser from the feedback of light reflected and scattered by the elements of the experimental system. The laser wavelength was tuned to the wing of the absorption profile. If the wavelength was tuned to its centre, the laser light was almost entirely absorbed in the vicinity of the entrance window of the cell. A long-time-scale drift of ECDL wavelength was continuously monitored by the photodiode and the CCD camera while observing resonance fluorescence $4^2P \rightarrow 4^2S$ at a side of the fluorescence cell. The stability of the wavelength due to the stable current supply and the temperature control, appeared sufficient, and no active stabilisation was needed. A Lumonics HD-500 dye laser pumped by an EX-520 excimer laser produced pulses of light of several nanosecond duration, exciting the second step (quadrupole-) transition to the states n^2F, with $n = 6, 7, 8$, at 528.7, 506.9, and 493.7 nm, respectively. The Coumarin 503 dye was used. The dye laser linewidth was *ca.* 4 GHz. The beams of both lasers were linearly polarised along the vertical axis. The fluorescence from the n^2F states, emerging through the glass cylinder of the cell was observed in the horizontal plane in the direction perpendicular to the laser beams. With the polariser across the fluorescence beam set at 54.7° from the vertical orientation, a "magic angle" configuration was set up to enable the observation of the population and not of the alignment (e.g. [24]). The fluorescence lines $n^2F \rightarrow 3^2D$ (with fine structure unresolved) at 960 nm, 890 nm, and 850 nm for $n = 6$, 7, and 8, respectively were selected with the help of a Carl Zeiss Jena SPM2 monochromator with spectral resolution of 4 nm per 1 mm of the slit. The fluorescence was collected by a 1:2 lens optical system into the entrance slit of the monochromator. The slits were set parallel to the axis of the laser beams and they were kept wide open (to 1.5 mm) to minimise the thermal escape effect [25]. The temporal development of the $n^2F_{5/2,7/2} \rightarrow 3^2D_{3/2,5/2}$ fluorescence decay was detected by using a photon counting system including a FEU 83 photomultiplier and an EG&G PAR 914P multichannel scaler (5 ns channel width). The S1 photocathode of the photomultiplier was cooled with LN_2 vapour to *ca.* 200 K. The FWHM of the laser pulse, as detected by the system, was *ca.* 10 ns, giving an effective measure of the temporal resolution of the system resulting from the length of the laser pulse, temporal response of the photomultiplier and the resolution of the multichannel scaler.

Effective lifetimes τ_{eff}, shortened by collisional quenching, were obtained from the experimental fluorescence decay signals by numerical fitting. After each

fluorescence decay, the noise was registered under the same conditions, but with the laser detuned by 1 cm^{-1} from the line. In this way the nonuniformity in time of the noise background was monitored, since it might arise from e.g. electrical noise from the excimer laser and/or by admixture of delayed fluorescence from the n^2F state populated via the $(n+1)^2D$ state excited from the $4^2P_{3/2}$ state by dye laser ASE. Such nonuniformity was usually hardly discernible, but before fitting, the noise signal was subtracted from the corresponding fluorescence signal. An example of an experimental decay is shown in Fig. 3. A sum of an exponential function

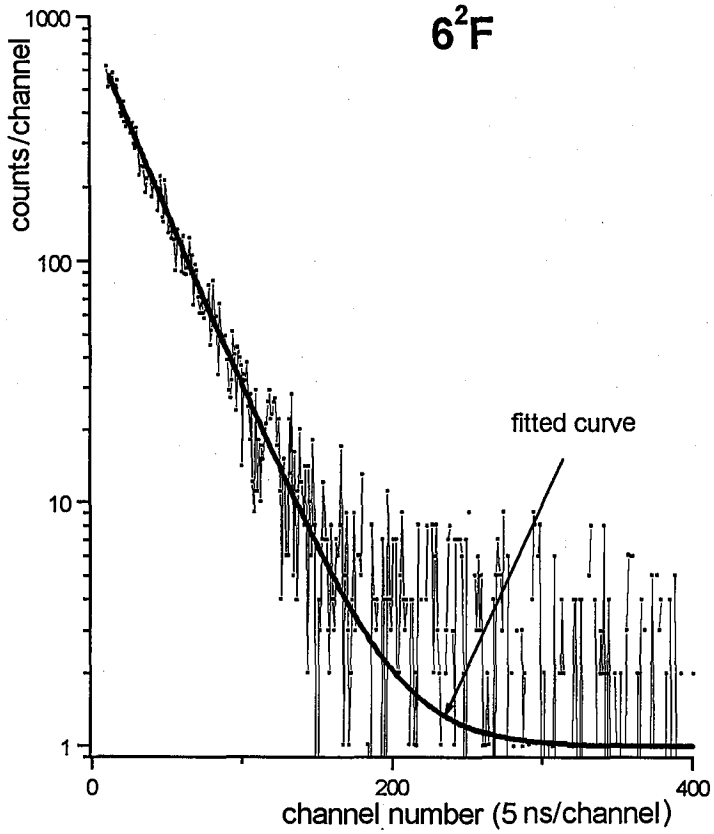

Fig. 3. An example of a registered fluorescence decay from the K(6^2F) state and the fitted curve (a sum of an exponential function and a constant, the letter representing the residual noise background, see the text).

and a constant (representing the residual noise background) was fitted. At a temperature of the experiment corresponding to a certain value of Nv (where N is the number density of the ground state K atoms and $v = (8kT/\pi\mu)^{1/2}$ is the mean relative velocity of the colliding atoms) the cross sections $\sigma_{l-\mathrm{mix}}$ were determined from the Stern–Volmer relation

$$1/\tau_{\mathrm{eff}} = 1/\tau_{\mathrm{rad}} + \sigma_{l-\mathrm{mix}} N v. \tag{3}$$

For the radiative lifetimes τ_{rad} the theoretical values of Theodosiou, corrected for the interaction of atoms with the thermal radiation, were taken from Ref. [26]. Often with collisional cross sections also the experimental lifetimes are determined by repeating measurements at various temperatures and by extrapolating, according to (3), the values of $1/\tau_{\text{eff}}$ corrected at each temperature for thermal radiation, to the collisionless limit of $Nv = 0$. Unfortunately this procedure was not possible under the conditions of our experiment since the range of temperatures at which we could perform the experiment was quite limited. We therefore assumed the theoretical value for lifetime taken from the literature.

3. Results and discussion

The results of our experiment are presented in the Table (and in Fig. 4). In the absence of theoretical treatment of these cross sections, we compare them with geometrical cross sections, defined as $\sigma_{\text{geom}} = \pi\left(\langle r_{nF}^2\rangle + 2\langle r_{nF}\rangle\langle r_{4S}\rangle + \langle r_{4S}^2\rangle\right)$ with mean radii $\langle r\rangle = n^{*2}\left\{1 + \frac{1}{2}\left[1 - l(l+1)/n^{*2}\right]\right\} a_0$ and mean square radii $\langle r^2\rangle = \frac{1}{2}n^{*2}\left[5n^{*2} + 1 - 3l(l+1)\right] a_0^2$, from hydrogenic expectation values for respective n^*. For alkali atom F states $n^* \cong n$; a_0 is the Bohr radius. In Fig. 4, together with our measured cross sections for K, other experimental results for l-mixing in collisions with parent ground state atoms, for F states in Rb from [1] and in Cs from [2], are plotted as a function of n, in a log–log scale. The geometrical cross sections, which are practically the same for all three elements, are marked by full circles, connected with a line to guide the eye. They scale nearly as n^4. The values for Rb, as mentioned in the introduction, were compared in [1] with the respective theoretical ones. They fall well within the limits embracing the geometrical cross sections, predicted for Rb by the de Prunelé–Pascale model approach, but coincide better with the lower limit, being systematically smaller than the geometrical cross sections. Our results for K are close to the respective geometrical cross sections. The results for Cs exceed σ_{geom} by an order of magnitude. As far as we know, there has been no theoretical attempt to explain such large values.

TABLE

Experimental l-mixing cross sections $\sigma_{l-\text{mix}}$ for the $K(n^2F)$ states, and corresponding geometrical cross sections σ_{geom}, in units of 10^{-13} cm^2.

Potassium states	$\sigma_{l-\text{mix}}$	σ_{geom}
6^2F	3.6 ± 2.2	2.7
7^2F	4.2 ± 2.6	5.1
8^2F	8.0 ± 4.6	8.8

In conclusion, our measured l-mixing cross sections for $K(n^2F)$ states contribute to the set of experimental data concerning l-mixing in alkali atoms due to

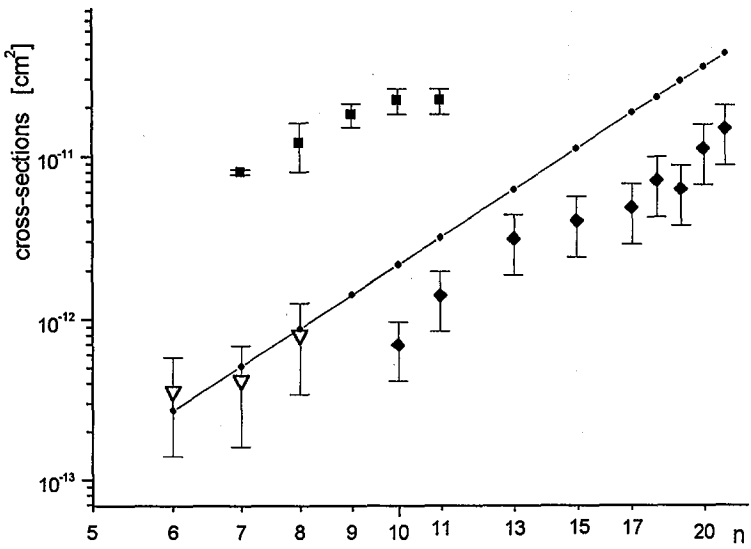

Fig. 4. Experimental cross sections for l-mixing of alkali n^2F states in thermal collisions with parent ground state atoms: ∇ — K (this work), ◆ — Rb (Ref. [1]), ■ — Cs (Ref. [2]). The full circles are for the geometrical cross sections.

thermal collisions with parent ground state atoms. Results of such excitation transfer in alkali–alkali collisions are not well represented in the literature, especially for relatively low ^2F levels and, to our best knowledge, have not been investigated earlier for the K(n^2F) states. The values obtained here are close to the geometrical cross sections, which are defined mainly by the size of the cloud of the excited state electron. This might suggest that the interaction of the perturber with the excited electron prevails in the studied collisional process. However a judgement as to the nature of the interactions involved will be possible only after a quantitative theoretical treatment of the case of potassium–potassium collisions is available. Especially that, from the results of calculations concerning alkali–noble gas collisions ([11] and references), there are indications that for all n-values, the interaction with the core may be of importance.

Although the assumption that collisional quenching of the investigated K(n^2F) states leads mostly to quasi-elastic transfer to the n, $l > 3$ levels of high multiplicity seems well grounded, it would be of interest to provide experimental evidence concerning the actual contribution to the measured cross section from quenching by the inelastic channels to the states outside a given n, $l \geq 3$ quasi-hydrogenic manifold.

Acknowledgments

This work was partially supported by the Committee for Scientific Research (Poland) (grant No. 2 P03B 065 11) and by the Latvian Science Council (grant No. 96.0609).

References

[1] M. Hugon, F. Gounand, P.R. Fournier, J. Berlande, *J. Phys. B* **12**, 2707 (1979).

[2] J. Marek, M. Ryschka, *Phys. Lett. A* **74**, 51 (1979).

[3] T.F. Gallagher, S.A. Edelstein, R.M. Hill, *Phys. Rev. Lett.* **35**, 644 (1975); T.F. Gallagher, S.A. Edelstein, R.M. Hill, *Phys. Rev. A* **15**, 1945 (1977).

[4] T.F. Gallagher, W.E. Cooke, S.A. Edelstein, *Phys. Rev. A* **17**, 904 (1978).

[5] M. Hugon, B. Sayer, P.R. Fournier, F. Gounand, *J. Phys. B* **15**, 2391 (1982).

[6] M. Chapelet, J. Boulmer, J.C. Gauthier, J.F. Delpech, *J. Phys. B* **15**, 3455 (1982).

[7] B. Dubreuil, C. Chaleard, *Phys. Rev. A* **29**, 958 (1984).

[8] V. Horvatic, M. Movre, C. Vadla, *J. Phys. B* **30**, 4943 (1997).

[9] A.P. Hickman, R.E. Olson, J. Pascale, in: *Rydberg States of Atoms and Molecules*, Eds. R.F. Stebbings, F.B. Dunning, Cambridge University Press, Cambridge 1982, p. 187.

[10] I.L. Beigman, V.S. Lebedev, *Phys. Rep.* **250**, 95 (1995).

[11] H. Liu, B. Li, *J. Phys. B* **27**, 497 (1994).

[12] F. Gounand, J. Berlande, in: *Rydberg States of Atoms and Molecules*, Eds. R.F. Stebbings, F.B. Dunning, Cambridge University Press, Cambridge 1982, p. 229.

[13] T.F. Gallagher, *Rep. Prog. Phys.* **51**, 143 (1988).

[14] I.I. Fabrikant, *Phys. Rev. A* **45**, 6404 (1992).

[15] E. de Prunelé, J. Pascale, *J. Phys. B* **12**, 2511 (1979).

[16] J. Szonert, B. Bieniak, M. Głódź, M. Piechota, *Z. Phys. D* **33**, 177 (1995).

[17] P.F. Liao, J.E. Bjorkholm, *Phys. Rev. Lett.* **36**, 1543 (1976).

[18] B. Bieniak, K. Fronc, M. Głódź, J. Szonert, *Opt. Appl.* **25**, 15 (1995).

[19] J. Marek, P. Münster, *J. Phys. B* **13**, 1731 (1980).

[20] H. Lundberg, S. Svanberg, *Z. Phys. A* **290**, 127 (1979).

[21] A. Ekers , M. Głódź, J. Szonert, B. Bieniak, K. Fronc, T. Radelitski, *Europ. Phys. J. D* **8**, 49 (2000).

[22] B. Bieniak, K. Fronc, S. Gateva-Kostova, M. Głódź, V. Grushevsky, J. Klavins, K. Kowalski, A. Rucińska, J. Szonert, *Phys. Rev. A* **62**, 022720 (2000).

[23] A.N. Nesmeyanov, *Vapor Pressure of the Chemical Elements*, Elsevier, Amsterdam 1963.

[24] P. Hannaford, R.M. Lowe, *Opt. Eng.* **22**, 532 (1983).

[25] L.J. Curtis, P. Erman, *J. Opt. Soc. Am.* **67**, 1218 (1977).

[26] C.E. Theodosiou, *Phys. Rev. A* **30**, 2881 (1984).